ROSE/TN/2002-01

The annealing of interstitial carbon atoms in high resistivity n-type silicon after proton irradiation

M. Kuhnke [a,*], E. Fretwurst [b], G. Lindstroem [b]

[a] *Department of Electronic and Computer Engineering, Brunel University, Howell Building, Middlesex UB8 3PH, United Kingdom*

[b] *II. Institut für Experimentalphysik, University of Hamburg, DESY Bldg. 67b, Luruper Chaussee 149, D-22761 Hamburg, Germany*

Abstract

The annealing of interstitial carbon C_i after 7-10 MeV and 23 GeV proton irradiations at room temperature in high resistivity n-type silicon is investigated. Deep level transient spectroscopy is used to determine the defect parameters. The annealing characteristics of the impurity defects C_i, C_iC_s, C_iO_i and VO_i suggest that the mobile C_i atoms are also captured at divacancy VV sites at the cluster peripheries and not only at C_s and O_i sites in the silicon bulk. The deviation of the electrical filling characteristic of C_i from the characteristic of a homogeneously distributed defect can be explained by an aggregation of C_i atoms in the environment of the clusters. The capture rate of electrons into defects located in the cluster environment is reduced due to a positive space charge region surrounding the negatively charged cluster core. The optical filling characteristic of C_i suggests that the change of the triangle shaped electric field distribution in a reverse biased p^+n junction due to charged clusters is negligible.

Key words: Silicon detectors, Radiation damage, Radiation hardness, DLTS
61.82.Fk, 81.40.Wx

* Cor. Author: Tel.: +44 1895 203199 ; E-mail: martin.kuhnke@brunel.ac.uk

1 Introduction

Recent experimental studies have shown oxygen enriched silicon detectors to be more radiation harder in charged particle environments compared to silicon detectors processed on standard FZ silicon [1]. A simulation of the defect kinetics during ^{60}Co γ-photon irradiation is feasible [2]. It is demonstrated the generation of the radiation-induced defects to depend on the oxygen and carbon concentrations. The hypothetical deep acceptor defect V_2O is employed to explain the different radiation tolerances of various silicon materials. The simple model predicts well the radiation hardness of oxygen-rich silicon and the deteriorate effect of carbon on the radiation hardness [3]. However, the simulation of the radiation damage during ^{60}Co γ-photon irradiation is more readily accomplished, since only single displacements of silicon atoms occur and the point defects are distributed homogeneously in the sample volume, while after particle irradiation in addition dense displacement regions are created [4]. The cluster damage affects the properties of silicon detectors, but it is independent on the impurity content. Thus, only after charged particle irradiations the beneficial effect of oxygen on the radiation hardness is revealed, since the generation of single displacements is higher for charged particles than for neutrons due to Coulomb scattering. Furthermore, it is suggested the cluster damage to influence the defect kinetic of the point defects, e.g. the build up of an impurity-defect shell around the clusters [5,6]. The DLTS method is applied to study the microscopic properties of the radiation-induced defects after low and high energy proton irradiations in more detail [7].

2 Experimental Procedures

One sample of 4kΩcm n-type FZ silicon was irradiated with 23 GeV protons and four samples of 2kΩcm n-type FZ silicon with 7-10 MeV protons. The equivalent fluence of the 23 GeV proton irradiation is $\Phi_{eq} = 10^{11}$ cm^{-2} and the particle fluence of the 7-10 MeV proton irradiations is $\Phi_p = 5 \cdot 10^{10}$ cm^{-2}. The impurity content in the 23 GeV proton irradiated sample is [P] $= 1.7 \cdot 10^{12}$ cm^{-3}, [O] $= 9.0 \cdot 10^{15}$ cm^{-3} and [C] $= 6.2 \cdot 10^{15}$ cm^{-3} and in the 7-10 MeV proton irradiated samples [P] $= 2.3 \cdot 10^{12}$ cm^{-3}, [O] $= 9.0 \cdot 10^{15}$ cm^{-3} and [C] $< 3.0 \cdot 10^{15}$ cm^{-3}. Simple p^+-n-n^+ structures with a guard ring were employed. The area of the p^+ region is 5x5 mm^2. The thickness of the samples is about 300 μm. The irradiated diodes were tempered for 80 min at 60°C or 4 min at 80°C to avoid any differences in the annealing state after irradiation. In both sample types the C_i annealing was not finished after the tempering step because of the low oxygen and carbon content.

A commercially available DLTS apparatus was employed for defect characterization which is described in more detail elsewhere [8]. For the sampling of the capacitance transients the time windows of 20 ms, 200 ms and 2 s were used. The digitized transients were weighted with 18 different functions. The b_1 coefficient, which corresponds to the sine wave weighting function, is taken to display the DLTS spectra. The reverse bias was 10 V and during filling with electrons a filling pulse 0 V was applied to the diode. During the filling with holes the forward bias was -3 V. Both types of filling pulses had a duration of 100 ms. For the capture measurements the duration of the electrical filling pulses was varied from 1 μs to 1 s. The optical filling was done by back side illumination of the reverse biased diode with an infrared LED ($\lambda_{max} = 880$ nm). Therefore, the ratio of the electron and hole concentrations in the space charge region was n/p $\ll 1$.

3 Experimental Results

The DLTS spectra of the 23 GeV proton irradiated sample during room temperature annealing are shown in Fig. 1. The annealing of C_i atoms is apparent. In Fig. 2 the dependence of the concentrations of the impurity defects C_i, C_iC_s, C_iO_i and VO_i on the annealing time t_a is shown. The sum of the defect concentrations is constant. One notes that the concentrations refer to a homogeneous distribution of defects. If the defects are concentrated in homogeneously distributed regions, the local concentration is larger than the averaged concentration assuming a homogeneous distribution of defects. In Fig. 3 the filling characteristics of $VO_i^0 \rightarrow VO_i^-$ and $C_iC_s(B)^0 \rightarrow C_iC_s(A)^-$ after 10 MeV proton irradiation are shown. The long filling time of C_iC_s arises from the configurational change $C_iC_s(B)^- \rightarrow C_iC_s(A)^-$. The defect is filled in configuration B and changes than to configuration A. The electron emission from the charge state $C_iC_s(B)^-$ is not detected, because its emission rate is much greater than the emission rate of $C_iC_s(A)^-$ at $T = 75$ K [9]. The filling characteristics indicate an increase of both defect concentrations. After 7, 8 and 9 MeV and 23 GeV proton irradiations the same effect is observed. Thus it is argued the mobile C_i atoms to be not solely trapped at C_s and O_i sites, forming C_iC_s and C_iO_i defects, but also at VV sites located at the cluster peripheries. The clusters are assumed to contain almost divacancies. The defect pair VC_s is considered to be unstable at room temperature, since this defect is similar to a single vacancy V in the silicon lattice. The released vacancies are captured at O_i sites outside the cluster regions, forming VO_i defects. At the cluster peripheries new C_s sites are generated, at which further C_i atoms are captured. Indeed, the trapping of C_i atoms at VV sites was already supposed in Ref. [9]. An increase of the concentration of C_iC_s accompanied by a decrease of the concentration of VV was observed. However, the concentration of divacancies in the clusters decreases only slightly during C_i annealing, as Fig. 1

illustrates. On the other hand site, the determination of the concentration of cluster defects from the DLTS spectra may be not very reliable.

In Fig. 4 the electrical filling characteristics of $C_i^0 \rightarrow C_i^-$ in the 23 GeV proton irradiated sample are shown. The characteristics deviate from the simulated one with a constant capture rate [10]. No dependence on the annealing state is seen. This suggests that the C_i atoms are localized in the environment of the clusters and hence the capture rate of majority charge carriers is reduced due to a positive space charge region surrounding the negatively charged cluster core [11]. The effect is less conspicuous after 7-10 MeV proton irradiation. In Fig. 5 the optical filling characteristic of $C_i^0 \rightarrow C_i^+$ in the 23 GeV proton irradiated sample is shown. The capture characteristic is described well by the simulated one assuming a constant capture rate [12]. For the calculation of the hole density distribution in the space charge region of the reverse biased p^+n junction one assumes a triangle shaped electric field distribution. The fitting of the measured and calculated signals supposes that the fraction of negatively charged divacancies in the clusters does not alter appreciably the electric field distribution. The hole capture cross-section is $\sigma_c = 1.30 \cdot 10^{-15}$ cm^2, which agrees reasonably with the cross-section $\sigma_T = 1.77 \cdot 10^{-15}$ cm^2 obtained from the DLTS spectra. Moreover, the result is reproducible for the optical capture characteristic of $C_iO_i^0 \rightarrow C_iO_i^+$ and for the 7-10 MeV proton irradiations. At $T = 180$ K the optical capture characteristic of $C_iO_i^0 \rightarrow C_iO_i^+$ was measured. The mean values of the hole capture cross-sections of the donor states are $\sigma_{Ci} = 1.37 \pm 0.08 \cdot 10^{-15}$ cm^2 and $\sigma_{CiOi} = 2.35 \pm 0.66 \cdot 10^{-16}$ cm^2. The ratios σ_c/σ_T are 0.91 ± 0.13 for the defect C_i and 0.83 ± 0.23 for the defect C_iO_i. One remarks that the temperature dependence of the effective masses is regarded for the calculations [13].

4 Conclusion

The experimental results demonstrate that the migration of C_i atoms is affected by strain and deformation fields originating from the clusters. The C_i atoms generated by the exchange reaction $I + C_s \rightarrow C_i$ are attracted to the cluster regions and their final migration volume is constricted to the neighbourhood of the clusters. This assumption is supported by the decrease of the capture rate of $C_i^0 \rightarrow C_i^-$ due to a positive space charge region surrounding the negatively charged cluster core of divacancies. The C_i atoms are captured at O_i and C_s sites in the cluster environment and also at VV sites at the cluster periphery. The released vacancies are captured at O_i sites outside the cluster regions. At the cluster peripheries new C_s sites are generated at which further C_i atoms are trapped. Thus the defect concentrations of the defects C_iC_s, C_iO_i and VO_i increase during C_i annealing and an envelope of C_iC_s defects can be formed around the clusters.

5 Acknowledgements

Support from the European Commission contract No. ERBFMRX-CT98-0208 is greatly appreciated.

References

[1] G. Lindström et al. Nucl. Instr. and Meth. **A465** (2001) 60

[2] K. Gill et al. J. Appl. Phys. **82** (1) (1997) 126 and Erratum J. Appl. Phys. **85** (11) (1999) 7990

[3] B.C. MacEvoy et al. Solid State Phenomena Vols. **57-58** (1997) 221

[4] V.A.J. van Lint et al. IEEE **NS-19** (6) (1972) 181

[5] A.V. Vasil'ev et al. Sov. Phys. Semicond. **16** (1) (1982) 84

[6] I.V. Antonova et al. Sov. Phys. Semicond. **23** (6) (1989) 671

[7] D.V. Lang J. Appl. Phys. **45** (7) (1974) 3023

[8] Dr. L. Cohausz PhysTech GmbH, Moosburg

[9] L.W. Song et al. Phys. Rev. **B42** (9) (1990) 5765

[10] D. Pons J. Appl. Phys. **55** (10) (1984) 3644

[11] B.R. Gossik J. Appl. Phys. **30** (8) (1959) 1214

[12] M. Kuhnke Ph.D. thesis, DESY-Report, University of Hamburg (2001)

[13] M.A. Green J. Appl. Phys. **67** (6) (1990) 2944

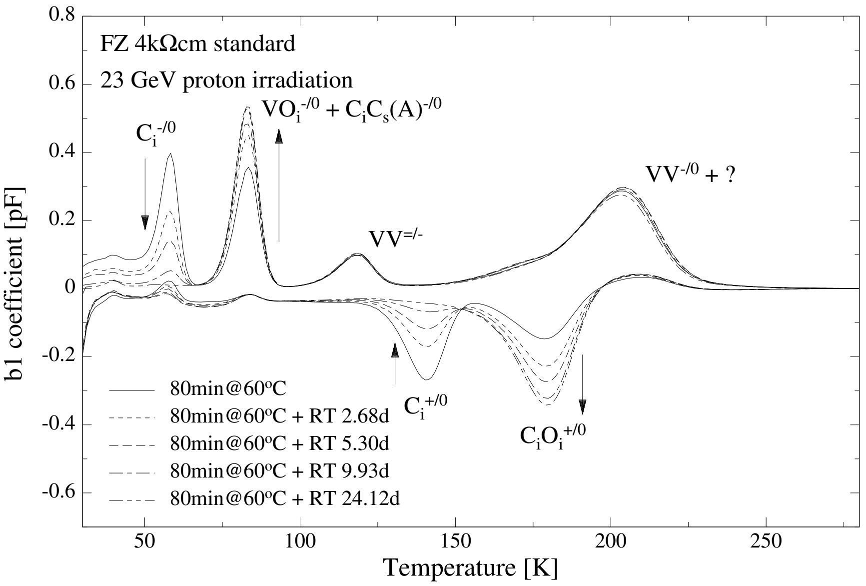

Fig. 1. The DLTS spectra of the 23 GeV proton irradiated sample during room temperature annealing are shown. The charge state transitions of the various radiation-induced defects are assigned to the DLTS signals. The arrows indicate the increase and decrease of the defect concentrations. Before room temperature annealing the sample was tempered for 80 min at 60°C.

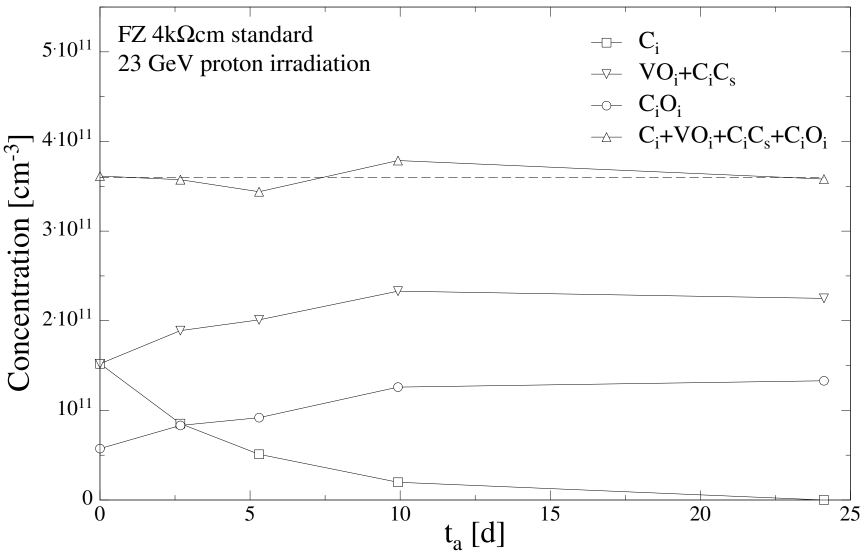

Fig. 2. The concentrations of the impurity defects during room temperature annealing in the 23 GeV proton irradiated sample are shown. Before room temperature annealing the sample was tempered for 80 min at 60°C.

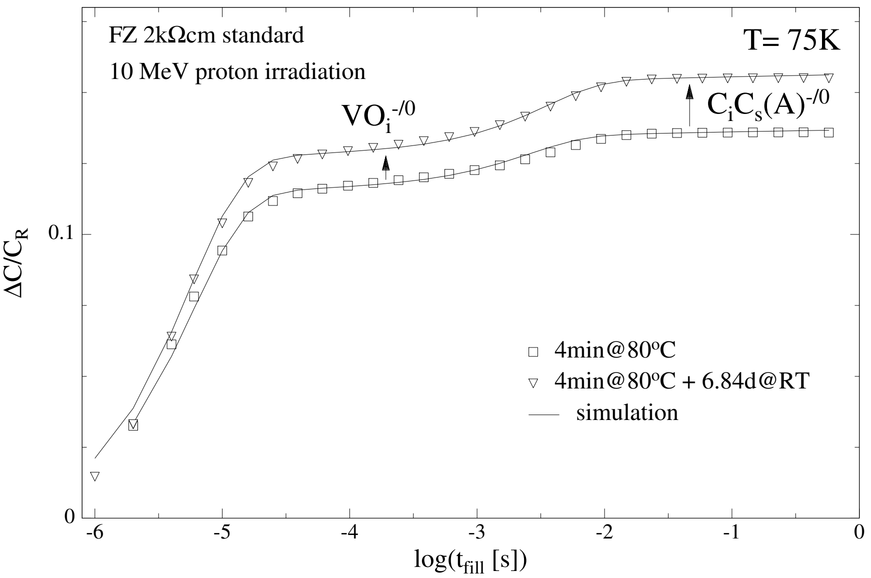

Fig. 3. The electrical filling characteristics of the defects VO_i and C_iC_s in the 10 MeV proton irradiated sample at two different annealing states are shown (symbols). The signal amplitudes of VO_i and C_iC_s increase. Also the simulated capture characteristics are shown (line).

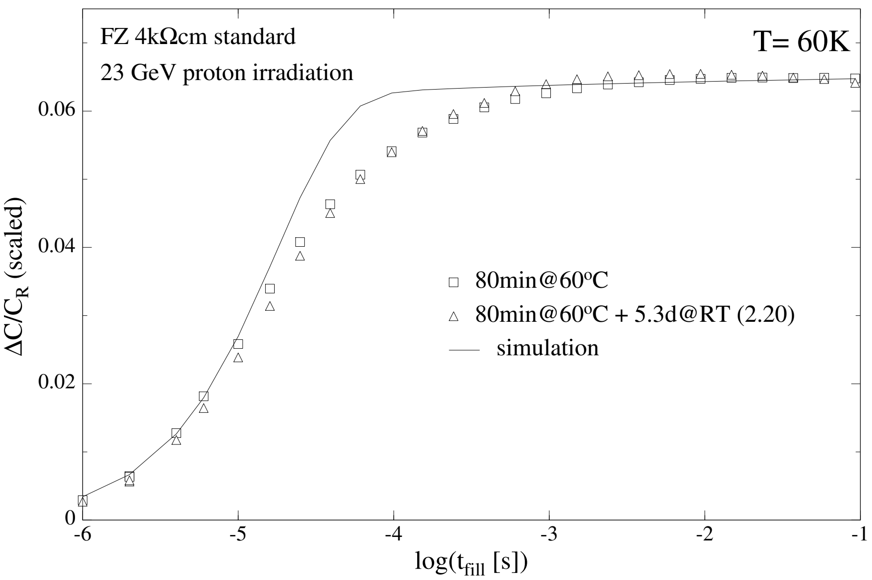

Fig. 4. The electrical filling characteristics of the defect C_i in the 23 GeV proton irradiated sample at two different annealing states are shown (symbols). The signal is scaled with the factor in the parenthesis. Also the simulation of the capture characteristic is shown (line).

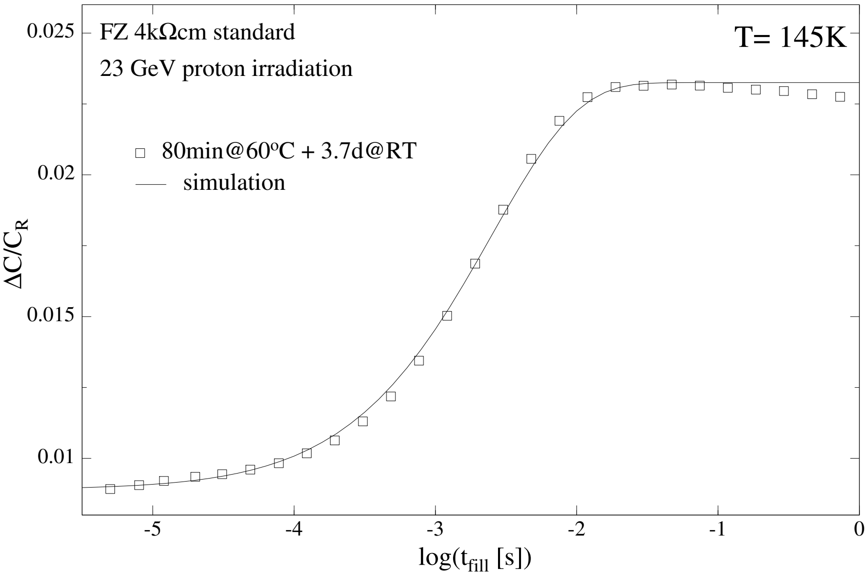

Fig. 5. The optical filling characteristic of the defect C_i in the 23 GeV proton irradiated sample is shown (symbols). Also the simulation of the capture characteristic is shown (line).